

# Crystal Structure and Chelate Ring Pucker of Bidentate (Pyrophosphato)tetraaquo chromium(III) Trihydrate, A Model for Metal-ADP Coordination

E. A. Merritt, M. Sundaralingam,\* and D. Dunaway-Mariano

Contribution from the Department of Biochemistry, University of Wisconsin, Madison, Wisconsin 53706, and the Department of Chemistry, University of Maryland, College Park, Maryland 20742. Received August 18, 1980

**Abstract:** Crystals of  $\alpha,\beta$ -bidentate  $\text{Cr}(\text{H}_2\text{O})_4\text{HP}_2\text{O}_7 \cdot 3\text{H}_2\text{O}$  are triclinic,  $P\bar{1}$ ,  $a = 7.038$  (1) Å,  $b = 8.858$  (1) Å,  $c = 10.636$  (1) Å,  $\alpha = 69.19$  (1)°,  $\beta = 89.54$  (1)°,  $\gamma = 68.37$  (1)°,  $Z = 2$ ,  $D_{\text{calc}} = 2.161 \text{ Mg m}^{-3}$ , and  $R = 0.063$  for 2401 unique reflections. This compound is one of a series of metal polyphosphate structures which serve as models for the metal phosphate coordination of biological complexes such as MgADP. While the previous compounds in this series have been cobalt-ammine complexes, this structure contains a chromium ion with water rather than ammonia in the coordination sphere. The six-membered chelate ring is in a boat conformation stabilized by crystal-packing interactions and is without the interligand hydrogen bonding seen in the corresponding cobalt-ammine complex  $\text{Co}(\text{NH}_3)_4\text{HP}_2\text{O}_7 \cdot 2\text{H}_2\text{O}$ .

The successful use of substitution-inert metal-nucleotide complexes such as  $\text{Co}(\text{NH}_3)_n\text{ATP}$  and  $\text{CrATP}$  to investigate the substrate specificity of enzymes which normally recognize  $\text{MgATP}^{1-3}$  has stimulated us to undertake the study of the metal phosphate coordination. We have previously reported the crystal structures of a series of (polyphosphato)cobalt-ammine complexes and used them to generate models of metal-nucleotide substrate conformations.<sup>4-6</sup> In the present complex,  $\text{Cr}(\text{H}_2\text{O})_4\text{HP}_2\text{O}_7 \cdot 3\text{H}_2\text{O}$ , chromium replaces the cobalt ion and water rather than ammonia completes the octahedral coordination of the metal ion. Aside from being a fragment of  $\text{CrATP}$ , this complex has itself been shown to be a substrate for yeast inorganic pyrophosphatase.<sup>7</sup> Previous structural identification of (polyphosphato)chromium(III) complexes ( $\text{CrATP}$ ,  $\text{CrADP}$ ,  $\text{CrPPP}$ , etc.) was based on chromatographic behavior, spectra data other than NMR, and comparison to the corresponding cobalt-ammine complexes. The X-ray structure determination of  $\text{Cr}(\text{H}_2\text{O})_4\text{HP}_2\text{O}_7$  will serve as a foundation for further structural assignments of the series.

## Experiment Section

**Preparation.** A 250-mL sample of 20 mM  $\text{Na}_4\text{P}_2\text{O}_7$  was adjusted to pH 4 with Dowex 50-X2 ( $\text{H}^+$ ) resin, filtered, and then added to 250 mL of 20 mM  $[\text{Cr}(\text{H}_2\text{O})_4\text{Cl}_2]\text{Cl}$ . The resulting solution was cooled to 10 °C and adjusted to pH 5.3 with saturated  $\text{KHCO}_3$ . The reaction solution was stirred for Ca. 15 min at 25 °C, filtered to remove unwanted polymer, cooled to 4 °C, adjusted to pH 2 with 6 N HCl, and loaded on a 65 × 2 cm Dowex 50-X2 ( $\text{H}^+$ , 100-200 mesh) column. The column was eluted with  $\text{H}_2\text{O}$  at 4 °C. The unreacted PP and  $\text{Cr}(\text{PP})_2$  were eluted with the first void volume while the  $\text{CrPP}$  began eluting only after several void volumes of  $\text{H}_2\text{O}$  (yield 30-40%). Unreacted  $\text{Cr}(\text{H}_2\text{O})_6^{3+}$  remained adsorbed at the top of the resin bed, as did the  $\text{Cr}_2\text{PP}$  formed in the reaction. Upon storage at 4 °C for a period of 2-3 weeks concentrated samples of  $\text{CrPP}$  (ca. 30 mM) yielded dark green crystals ( $\lambda_{\text{max}} = 595 \text{ nm}$  ( $\epsilon = 24$ ),  $425 \text{ nm}$  ( $\epsilon = 25$ )).

**Structure Solution and Refinement.** Crystals belong to space group  $P\bar{1}$ , with  $a = 7.038$  (1) Å,  $b = 8.858$  (1) Å,  $c = 10.636$  (1) Å,  $\alpha = 69.19$  (1)°,  $\beta = 89.54$  (1)°,  $\gamma = 68.37$  (1)°, volume = 570.3 (2) Å<sup>3</sup>, and  $Z = 2$ . A total of 2401 unique intensities were collected by the  $\theta$ - $2\theta$  scan mode from a crystal measuring  $0.05 \times 0.1 \times 0.2 \text{ mm}$  by using nickel-filtered copper radiation ( $\lambda = 1.5418$  Å) on an Enraf-Nonius CAD4 diffractometer. No net drop was observed in the intensity of four standard reflections measured after every 2 h of X-ray exposure. Lorentz and polarization correction and an empirical absorption correction on the basis of the Eulerian angle  $\Phi$  were applied during data reduction.

The structure was solved by direct methods, and the 17 nonhydrogen atoms refined by block-diagonal least-squares by using anisotropic thermal parameters. The 15 hydrogen atoms were then located in successive difference Fourier syntheses. All atoms were refined by full-matrix least-squares including isotropic thermal parameters for the hy-

Table I. Positional and Isotropic Thermal Parameters for  $\alpha,\beta$ -bidentate  $\text{Cr}(\text{H}_2\text{O})_4\text{HP}_2\text{O}_7 \cdot 3\text{H}_2\text{O}^a$

	$x/a$	$y/b$	$z/c$	$B, \text{Å}^2$
Cr	0.73395 (8)	0.58492 (6)	0.72805 (5)	0.84 (1)
P(1)	0.3116 (1)	0.8149 (1)	0.7829 (1)	1.02 (2)
P(2)	0.3091 (1)	0.7632 (1)	0.5304 (1)	0.97 (2)
O(1)	0.5458 (4)	0.7460 (3)	0.8046 (2)	1.36 (5)
O(11)	0.2348 (4)	0.9876 (3)	0.8107 (3)	2.08 (6)
O(111)	0.2213 (4)	0.6896 (3)	0.8663 (3)	2.02 (7)
O(12)	0.2346 (4)	0.8777 (3)	0.6257 (2)	1.50 (6)
O(2)	0.5075 (4)	0.6074 (3)	0.6112 (2)	1.47 (6)
O(22)	0.3413 (4)	0.8870 (3)	0.4009 (3)	1.79 (6)
O(222)	0.1412 (4)	0.7019 (3)	0.5161 (3)	1.80 (6)
OW(1)	0.9269 (4)	0.4253 (3)	0.6536 (3)	1.84 (6)
OW(2)	0.9710 (4)	0.5404 (3)	0.8541 (3)	1.71 (6)
OW(3)	0.7775 (4)	0.7854 (3)	0.5964 (3)	1.79 (6)
OW(4)	0.6977 (4)	0.3832 (3)	0.8704 (2)	1.68 (6)
OW(5)	-0.1595 (5)	0.0705 (3)	-0.1603 (3)	2.00 (7)
OW(6)	-0.3377 (5)	0.6881 (3)	0.2864 (3)	2.27 (7)
OW(7)	0.2544 (5)	0.2076 (4)	0.9869 (3)	2.42 (7)
H(011)	0.090 (17)	1.042 (12)	0.820 (10)	10.9 (32)
H(1A)	1.060 (8)	0.389 (6)	0.672 (5)	2.1 (10)
H(1B)	0.893 (8)	0.391 (6)	0.601 (5)	2.0 (11)
H(2A)	1.042 (8)	0.436 (6)	0.894 (5)	1.9 (10)
H(2B)	1.027 (9)	0.613 (7)	0.830 (6)	2.8 (12)
H(3A)	0.910 (9)	0.760 (7)	0.556 (6)	3.0 (13)
H(3B)	0.727 (8)	0.893 (6)	0.590 (5)	2.1 (11)
H(4A)	0.698 (9)	0.359 (7)	0.961 (6)	2.8 (12)
H(4B)	0.739 (8)	0.290 (6)	0.863 (5)	2.1 (11)
H(5A)	-0.209 (14)	0.011 (11)	-0.103 (9)	8.2 (27)
H(5B)	-0.226 (10)	0.104 (8)	-0.239 (6)	3.8 (15)
H(6A)	-0.416 (10)	0.737 (7)	0.323 (6)	3.4 (14)
H(6A)	-0.361 (16)	0.600 (12)	0.326 (10)	7.3 (28)
H(7A)	0.327 (10)	0.216 (7)	1.031 (6)	3.4 (14)
H(7A)	0.337 (14)	0.223 (10)	0.904 (9)	7.0 (24)

<sup>a</sup> Thermal parameters given for nonhydrogen atoms are  $B_{\text{eq}}$ .

drogen atoms. Reflections were given weight  $w = (\sigma^2 + (0.02F_o)^2)^{-1}$ . Eight reflections exhibiting strong secondary extinction and 115 reflec-

(1) Abbreviations: ADP = adenosine 5'-diphosphate, ATP = adenosine 5'-triphosphate. In metal complexes such as MgATP where no explicit additional ligands are given the coordination sphere is assumed to be filled by water.

(2) Cornelius, R. D.; Cleland, W. W. *Biochemistry* 1978, 17, 3279.

(3) Dunaway-Mariano, D.; Cleland, W. W. *Biochemistry* 1980, 19, 1496, 1506.

(4) Merritt, E. A.; Sundaralingam, M.; Cornelius, R. D.; Cleland, W. W. *Biochemistry* 1978, 17, 3274.

(5) Merritt, E. A.; Sundaralingam, M. *Acta Crystallogr.* in press.

(6) Merritt, E. A.; Sundaralingam, M.; Cornelius, R. D. *J. Am. Chem. Soc.*, in press.

(7) Knight, W.; Dunaway-Mariano, D., unpublished results.

\* To whom correspondence should be addressed at the University of Wisconsin.

Table II. Bond and Torsion Angles (Deg) in  $\alpha,\beta$ -Bidentate  $\text{Cr}(\text{H}_2\text{O})_4\text{HP}_2\text{O}_7 \cdot 3\text{H}_2\text{O}^a$ 

O(1)-Cr-O(2)	91.9	O(2)-Cr-OW(4)	88.8
O(1)-Cr-OW(1)	178.6	OW(1)-Cr-OW(2)	88.0
O(1)-Cr-OW(2)	90.7	OW(1)-Cr-OW(3)	91.1
O(1)-Cr-OW(3)	88.5	OW(1)-Cr-OW(4)	90.3
O(1)-Cr-OW(4)	90.1	OW(2)-Cr-OW(3)	89.9
O(2)-Cr-OW(1)	89.5	OW(2)-Cr-OW(4)	87.1
O(2)-Cr-OW(2)	175.2	OW(3)-Cr-OW(4)	176.6
O(2)-Cr-OW(3)	94.3	O(11)-P(1)-O(111)	111.9
O(1)-P(1)-O(11)	105.7	O(11)-P(1)-O(12)	104.3
O(1)-P(1)-O(111)	115.3	O(111)-P(1)-O(12)	110.3
O(1)-P(1)-O(12)	108.7	O(2)-P(2)-O(22)	114.0
O(12)-P(2)-O(2)	105.1	O(2)-P(2)-O(222)	110.7
O(12)-P(2)-O(22)	104.7	O(22)-P(2)-O(222)	115.2
O(12)-P(2)-O(222)	106.2	O(12)-P(2)-O(2)-Cr	-36.7
Cr-O(1)-P(1)-O(12)	-46.0	P(2)-O(2)-Cr-O(1)	38.3
O(1)-P(1)-O(12)-P(2)	53.6	O(2)-Cr-O(1)-P(1)	9.8
P(1)-O(12)-P(2)-O(2)	-15.7		

<sup>a</sup> Mean esd for bond and torsion angles are 0.2 and 0.3°.

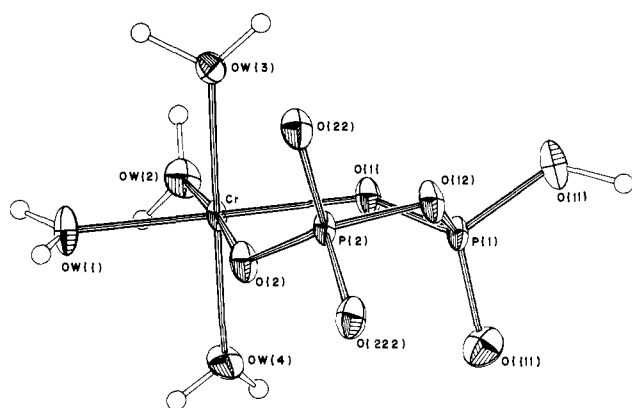


Figure 1. The  $\alpha,\beta$ -bidentate  $\text{Cr}(\text{H}_2\text{O})_4\text{HP}_2\text{O}_7$  complex with thermal ellipsoids drawn at the 50% probability level.

tions with  $F_o < 3\sigma(F_o)$  were given zero weight in the final cycles of the refinement. The final  $R$  index for the 2378 reflections was 0.060 and for all 2401 reflections, 0.063. At the conclusion of the refinement, the maximum shift/ $\sigma$  ratio was 0.3. Atomic scattering factors were taken from ref 8, including anomalous scattering components for all nonhydrogen atoms.

## Discussion

The  $\alpha,\beta$ -bidentate  $\text{Cr}(\text{H}_2\text{O})_4\text{HP}_2\text{O}_7$  complex is shown in Figure 1. The six-membered chelate ring Cr-O(1)-P(1)-O(12)-P(2)-O(2) formed by the bidentate phosphate coordination is in a boat conformation. It may be described by using the Cremer-Pople formalism<sup>7</sup> by the parameters  $Q = 0.575$  (3) Å,  $\phi = 306.7$  (3)°, and  $\theta = 96.2$  (4)°. Fractional atomic coordinates are given in Table I. Bond distances, bond angles, and torsion angles are given in Figure 2 and Table II. The pyrophosphate bond lengths and angles are very close to those in the (pyrophosphato)cobalt-ammine complex. The P-O bonds involving the bridge oxygen atom O(12) are again significantly asymmetric (P(1)-O(12) = 1.591 (2) Å; O(12)-P(2) = 1.631 (3) Å), with the shorter bond belonging to the protonated phosphate. Every hydrogen atom in the structure is involved in hydrogen bonding (Table III and Figure 3). The four liganded water molecules act solely as hydrogen-bond donors, while the three free waters each accept two hydrogen bonds as well. Pyrophosphate groups in neighboring molecules interact indirectly through chains of hydrogen bonded water molecules (Figure 3), the shortest chain

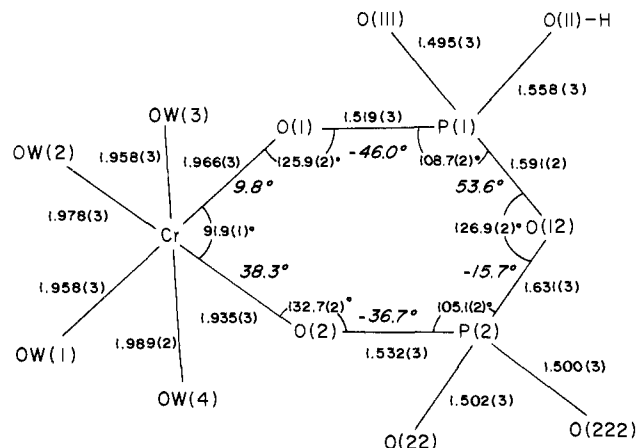


Figure 2. Bond distances and ring bond and torsion angles. Additional values are given in Table II.

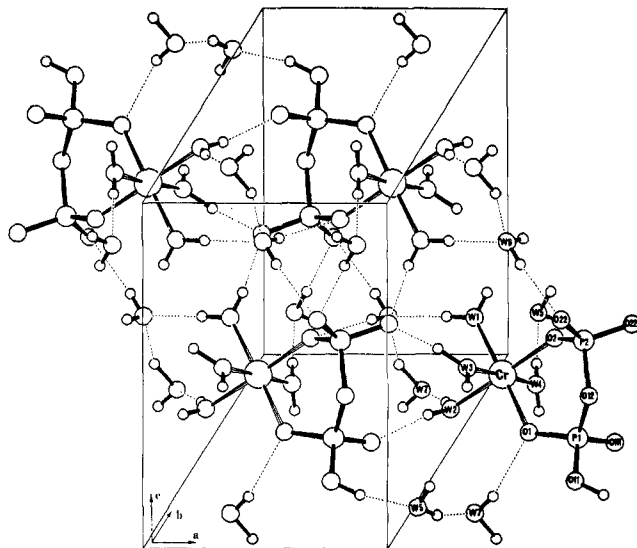


Figure 3. Crystal packing of  $\text{Cr}(\text{H}_2\text{O})_4\text{HP}_2\text{O}_7 \cdot 3\text{H}_2\text{O}$  with hydrogen bonding shown as dotted lines.

Table III. Hydrogen Bonding in  $\alpha,\beta$ -Bidentate  $\text{Cr}(\text{H}_2\text{O})_4\text{HP}_2\text{O}_7 \cdot \text{H}_2\text{O}^a$

hydrogen bond donor	H	acceptor	symmetry code	D...A, Å	H...A, Å	H...A, deg
OW(1)-H(1A)		...O(W6)	[2: 1,1,1]	2.685	1.82	179
OW(1)-H(1B)		...O(222)	[2: 1,1,1]	2.572	1.78	171
OW(2)-H(2A)		...OW(7)	[1: 1,0,0]	2.723	1.92	168
OW(2)-H(2B)		...O(111)	[1: 1,0,0]	2.590	1.83	150
OW(3)-H(3A)		...O(222)	[1: 1,0,0]	2.616	1.62	171
OW(3)-H(3B)		...O(22)	[2: 1,2,1]	2.719	1.87	170
OW(4)-H(4A)		...O(111)	[2: 1,1,2]	2.656	1.78	162
OW(4)-H(4B)		...OW(5)	[1: 1,0,1]	2.715	1.92	178
OW(5)-H(5A)		...OW(7)	[2: 0,0,1]	2.807	2.03	157
OW(5)-H(5B)		...O(22)	[2: 0,1,0]	2.709	1.87	165
OW(6)-H(6A)		...O(22)	[1: -1,0,0]	2.870	2.11	173
OW(6)-H(6B)		...O(2)	[2: 0,1,1]	3.119	2.32	163
OW(6)-H(6B)		...O(222)	[2: 0,1,1]	3.103	2.48	133
OW(7)-H(7A)		...O(1)	[2: 1,1,12]	2.861	2.15	161
OW(7)-H(7B)		...OW(6)	[2: 0,1,1]	2.848	1.90	149
O(11)-H(11)		...OW(5)	[1: 0,1,1]	2.642	1.70	161
mean esd				0.004	0.06	6

<sup>a</sup> Acceptor atom symmetry code is given as  $x, y,$  and  $z$  translation preceded by the symmetry operation as follows: (1)  $x, y, z$ ; (2)  $-x, -y, -z$ .

being O(11)-H...OW(5)-H...O(22).

The conformation of the chelate ring in this chromium complex is different than that observed for the two previous bidentate cobalt(III) model compounds<sup>5</sup>  $\alpha,\beta$ -bidentate  $\text{Co}(\text{NH}_3)_4\text{HP}_2\text{O}_7$ .

(8) "International Tables for X-ray Crystallography"; Kynoch Press: Birmingham, England, 1974; Vol. IV.

(9) Cremer, D.; Pople, J. A. *J. Am. Chem. Soc.* 1975, 97, 1354.

$2\text{H}_2\text{O}$  and ( $\Delta$ )- $\beta,\gamma$ -bidentate  $\text{Co}((\text{NH}_3)_4\text{H}_2\text{P}_3\text{O}_{10})\text{H}_2\text{O}$ . The two cobalt chelate rings are almost identical, differing chiefly in the amplitude of pucker:  $Q = 0.623 \text{ \AA}$  vs.  $Q = 0.503 \text{ \AA}$ , respectively. The amplitude of pucker in the present chromium complex is intermediate between the two cobalt complexes. However, the pseudorotation phase angle  $\phi$  is  $72^\circ$  and  $68^\circ$  in the two cobalt rings (twist boat), which allows the phosphate oxygens projecting axially from the ring to hydrogen bond across the top and bottom of the chelate ring to the axial ammine ligands. The N...O distances in these hydrogen bonds range from 3.003 to 3.116  $\text{\AA}$ . Instead the chromium ring is  $120^\circ$  away on the pseudorotation cycle at  $\phi = 306.7 (3)^\circ$ , which precludes the formation of interligand hydrogen bonds. The principal factor affecting the cobalt-ammine chelate ring conformation in the crystal structures is the interligand hydrogen bonding just mentioned. In solution the chromium complex may also assume a conformation stabilized by interligand hydrogen bonding with pseudorotation phase  $\phi$  similar to the cobalt-ammine complexes. To do so, however, the chelate ring would have to increase its amplitude of pucker to bring the interligand separation into O...O hydrogen-bonding distance.

The six-membered chelate ring in these complexes is free to pseudorotate along the cycle of boat and twist-boat conformations. The energetically favored conformations along this path are determined by the hydrogen-bonding environment. When the axial position in the metal's coordination sphere can be occupied by nitrogen, as in the cobalt-ammine complexes, or when the metal is complexed with functional groups at an enzyme's substrate-binding site, then the possibility of stabilizing N...O hydrogen bonding across the top and bottom of the ring favors the twist-boat conformations at  $\phi = 70^\circ$  and  $\phi = 250^\circ$ .<sup>4</sup> When the axial ligands are waters the enzyme could introduce strain in the phosphodiester bonds by increasing the amplitude of ring pucker, thus shortening the distance from the phosphate oxygens to the axial water ligands to allow the formation of hydrogen bonds.

With magnesium substrates (MgPP, MgADP, MgATP), where the coordination half-life is short, a functional group from the

enzyme itself might replace an axially liganded water upon substrate binding. The enzyme functional group could then participate in interligand hydrogen bonding directly. This is not the case for the much more stable substitution-inert Co(III) and Cr(III) complexes, and enzymes for which these are acceptable substrates thus do not require such direct chelation to the metal. However, the enzyme may provide hydrogen-bond donors (or acceptors) which are not themselves liganded, and these may act to stabilize particular substrate conformations other than the twist-boat forms with attendant interligand hydrogen bonding. The extensive hydrogen-bonding network in the present structure may illustrate this. Evidence that the enzyme (kinases in the case of metal-ATP and pyrophosphatase in the case of metal-PP) does act as a hydrogen-bond donor in this fashion may be provided by the observation that the tetraamminecobalt and tetraamminechromium complexes bind very poorly to these enzymes on the whole,<sup>10</sup> while the tetraaquochromium complexes bind as tightly as the corresponding magnesium complexes.<sup>3</sup> The poorer binding may also be due to the liganded waters acting as acceptors for enzyme-donated hydrogen bonds, which the liganded ammonia cannot accept.

**Acknowledgment.** Research supported by NIH Grant GM-17378 to M.S. and NIH Biomedical Research Support Grant, University of Maryland, to D.D., who also acknowledges the Research Corp. and the donors of the Petroleum Research Fund, administered by the American Chemical Society, for partial support.

**Supplementary Material Available:** Listings of anisotropic thermal parameters and of structure factors (9 pages). Ordering information is given on any current masthead page.

(10) Janson, C. A.; Cleland, W. W. *J. Biol. Chem.* **1974**, *249*, 2562, 2567, 2572.

## Proton Nuclear Magnetic Resonance Study of the Relaxation Behavior and Kinetic Lability of Exchangeable Protons in the Heme Pocket of Cyanometmyoglobin

John D. Cutnell,<sup>1</sup> Gerd N. La Mar,\* and Stephen B. Kong

Contribution from the Department of Chemistry, University of California, Davis, California 95616. Received November 7, 1980

**Abstract:** The  $z$ -magnetization recovery times for several hyperfine-shifted exchangeable protons and the  $T_1$ 's for two heme methyl signals were determined for sperm whale metmyoglobin cyanide in  $\text{H}_2\text{O}$  solution. In the absence of saturation transfer from the suppressed  $\text{H}_2\text{O}$  signal, the determined recovery times for the exchangeable protons represent intrinsic  $T_1$ 's. The ratios of exchangeable proton  $T_1$ 's to methyl  $T_1$ 's yield relative  $r^{-6}$  values, which, with the known distance for the heme methyl, result in assignment of the exchangeable imidazole proton for the proximal and distal histidines, the proximal histidine peptide NH, and, most likely, the imidazole NH of His FG2. At  $40^\circ\text{C}$ , pH-dependent saturation transfer factors determined by Redfield experiments and line width analysis permitted the characterization of the exchange rates and mechanisms for the four assigned exchangeable protons. The dominant base-catalyzed proximal histidyl imidazole NH is consistent with the coordination of the imidazole to the iron. A dominant acid-catalyzed proton-exchange mechanism for the distal suggests a hydrogen bond to the coordinated cyanide ligand, which is also supported by the short distance of the exchangeable proton from the iron.

The investigation of numerous structure-function relationships in hemoproteins utilizing proton nuclear magnetic resonance is considerably simplified in the paramagnetic forms of these molecules. In this form, the short-ranged electron-nuclear interactions yield sizable hyperfine shifts which permit resolution

of the peaks for the nuclei at the active site.<sup>2</sup> Detailed interpretation of the hyperfine shifts and their dependence on physiological factors, however, depends critically on the unambiguous assignment of the resolved resonances. While this is readily

(1) On leave from the Department of Physics, Southern Illinois University, Carbondale, IL.

(2) Morrow, J. S.; Gurd, F. R. N. *CRC Crit. Rev. Biochem.* **1975**, *3*, 221-287; La Mar, G. N. In "Biological Applications of Magnetic Resonance"; Shulman, R. G., Ed.; Academic Press: New York, 1979; pp 305-343.